

Mkn 1239: A highly polarized NLS1 with a steep X-ray spectrum and strong NeIX emission ¹

D. Grupe² and S. Mathur

Astronomy Department, Ohio State University, 140 W. 18th Ave., Columbus, OH-43210, U.S.A.
 dgrupe, smita@astronomy.ohio-state.edu

S. Komossa

MPI für extraterrestrische Physik, Giessenbachstr. 1, D-85748 Garching, Germany
 skomossa@mpe.mpg.de

ABSTRACT

We report the results of an XMM-Newton observation of the Narrow-Line Seyfert 1 galaxy Mkn 1239. This optically highly polarized AGN has one of the steepest X-ray spectra found in AGN with $\alpha_X=+3.0$ based on ROSAT PSPC data. The XMM-Newton EPIC PN and MOS data confirm this steep X-ray spectrum. The PN data are best-fit by a powerlaw with a partial covering absorption model suggesting two light paths between the continuum source and the observer, one indirect scattered one which is less absorbed and a highly absorbed direct light path. This result agrees with the wavelength dependent degree of polarization in the optical/UV band. Residuals in the X-ray spectra of all three XMM-Newton EPIC detectors around 0.9 keV suggest the presence of an emission line feature, most likely the Ne IX triplet. The detection of NeIX and the non-detection of OVII/OVIII suggest a super-solar Ne/O ratio.

Subject headings: galaxies: active - quasars:general - quasars: individual (Mkn 1239)

1. Introduction

With the launch of the X-ray satellite ROSAT (Trümper 1982) the X-ray energy range down to 0.1 keV became accessible for the first time. During the half year ROSAT All-Sky Survey (RASS, Voges et al. (1999)) a large number of sources with steep X-ray spectra were detected (Thomas et al. (1998); Beuermann et al. (1999); Schwope et al. (2000)). About one third to one half of these sources are AGN. Grupe (1996) and Grupe et al. (1998a, 2004a) found that about 50% of bright soft X-ray selected AGN are Narrow-Line Seyfert 1 galaxies (NLS1s, Osterbrock & Pogge

(1985); Goodrich (1989)). They turned out to be the class of AGN with the steepest X-ray spectra (e.g. Boller et al. (1996); Grupe (1996); Grupe et al. (1998a); Grupe et al. (2001); Vaughan et al. (2001); Grupe et al. (2004a); Williams et al. (2002)). NLS1s are AGN with extreme properties which seem to be linked to each other: An increase in their X-ray spectral index α_X correlates with the strength of the optical FeII emission and anti-correlates with the widths of the Broad Line Region (BLR) Balmer lines and the strength of the Narrow-Line Region (NLR) forbidden lines (e.g. Grupe (1996); Grupe et al. (1999); Grupe (2004); Laor et al. (1994, 1997); Sulentic et al. (2000)). All these relationships are governed by one fundamental underlying parameter, usually called the Boroson & Green (1992) 'Eigenvector-1' relation in AGN. The most accepted explanation for Eigenvector 1 is the Eddington ratio L/L_{Edd} (Boroson

¹Based on observations obtained with XMM-Newton, an ESA science mission with instruments and contribution directly funded by ESA member states and NASA

²Guest observer, McDonald Observatory, University of Texas at Austin

2002; Sulentic et al. 2000; Grupe 2004; Yuan & Wills 2003) in which NLS1s are AGN with the highest Eddington ratios.

In a spectropolarimetry study of 18 NLS1s Goodrich (1989) found three sources to show significant polarization that allowed a detailed spectropolarimetric analysis: Mkn 766, Mkn 1239, and IRAS 1509–211. All these sources show an increase of the degree of polarization towards the blue. In the Broad Line Region (BLR) Balmer lines the degree of polarization is larger than in the continuum, while it is less in the Narrow Line Region (NLR) forbidden lines, suggesting the scattering medium is somewhere located between the BLR and NLR (e.g. Wills et al. (1992)). All three sources were observed with the Position Sensitive Proportional Counter (PSPC, Pfeffermann et al. (1987)) on board ROSAT (Rush et al. (1996a); Grupe et al. (1998b); Pfefferkorn et al. (2001)). The NLS1 Mkn 1239 ($\alpha_{2000}=09^{\text{h}} 52^{\text{m}} 19.1\text{s}$; $\delta_{2000} = -01^{\circ} 36' 43''$; $z=0.019$) had an unusually steep X-ray spectral index $\alpha_{\text{X}}=2.9$ (Boller et al. 1996) during the ROSAT pointed observation. Here we present the results of a serendipitous observation of Mkn 1239 with XMM-Newton (Jansen et al. 2001).

The outline of this paper is as follows: in § 2 we describe the XMM and ROSAT observations and the data reduction, in § 3 we present the results of the ROSAT and XMM data analysis, and in § 4 we discuss the results. Throughout the paper spectral indexes are denoted as energy spectral indexes with $F_{\nu} \propto \nu^{-\alpha}$. Luminosities are calculated assuming a Hubble constant of $H_0 = 75 \text{ km s}^{-1} \text{ Mpc}^{-1}$ and a deceleration parameter of $q_0 = 0.0$.

2. Observations

2.1. XMM-Newton Observation

Mkn 1239 was observed by XMM-Newton during orbit 353 on 2001-11-12 from UT 20:04 - 22:57 for 5 ks with the EPIC PN (Strüder et al. (2001)) and 9.4 ks with the EPIC MOS (Turner et al. (2001)) with the thin filters in Full Frame Mode. The background during the observation was low so all of the observing times were used.

Source photons were collected in a circle with a radius of $25''$. The background photons of the PN observation were collected in a circular region

close by with a radius of $50''$ and in the MOS observation of an annulus with an inner radius of $30''$ and an outer radius of $75''$. Only events with $\text{PATTERN} \leq 4$ for the PN and ≤ 12 for the MOS were selected for the spectral analysis with quality parameter $\text{FLAG}=0$. The count rates in all three EPIC detectors were low enough (see § 3.1) that the observations were not affected by pile-ups. Because it was a serendipitous observation, the source was not observed on CCD #1 in the MOS cameras, but instead on CCD #4 and #6 on MOS-1 and MOS-2, respectively. The position on the EPIC PN was on CCD #4 close to the CAMEX.

The XMM data were reduced by using the XMM-Newton Science Analysis Software (XMM-SAS) version 5.4.1 and the X-ray spectra were analyzed by XSPEC 11.2.0. The spectra were grouped by GRPPHA 3.0.0 in bins of at least 15 counts per bin. The response matrices and auxiliary response files were created for the XMM observations by the XMM-SAS tasks *rmfgen* and *arfgen*.

For the sake of completeness and comparison with the XMM data, we retrieved and reanalyzed the ROSAT PSPC data as well. Details of the ROSAT observations are given below.

2.2. ROSAT PSPC observations

Mkn 1239 was observed twice by ROSAT, first during the RASS (Rush et al. 1996a) and second in a pointed PSPC observation (Boller et al. 1996; Grupe et al. 1998b; Pfefferkorn et al. 2001). During the RASS coverage on 1990-11-13 to 1990-11-14 the source was observed for a total of 418s and the pointed ROSAT PSPC observation was performed on 1992-11-08 between UT 05:53 - 15:58 for a total of 9043 s (ROR 700908p, Pfefferkorn et al. (2001)). The source was on-axis. Source photons were collected in a circle with a radius of $100''$ and the background photons in a circular region close by with a radius of $200''$.

The ROSAT data were analyzed by both, the Extended X-ray Scientific Analysis System (EXSAS, Zimmermann et al. (1998)) version 01APR and XSPEC 11.2.0.. For the count-rate conversions between different X-ray missions, PIMMS 3.2 was used.

3. Results

3.1. X-ray variability

During its RASS and its pointed ROSAT PSPC observations Mkn 1239 had mean count rates of $0.054 \pm 0.014 \text{ cts s}^{-1}$ and $0.069 \pm 0.003 \text{ cts s}^{-1}$, respectively (Pfefferkorn et al. (2001)), suggesting no significant variability in the two years between the two ROSAT observations. On the other hand, the light curve of the pointed PSPC observation (Figure 1) suggests some variability by $\approx 25\%$ during the 10h coverage. The PSPC hardness ratios³ were 0.81 ± 0.18 and 0.29 ± 0.10 during the RASS and pointed PSPC observations suggesting a change in the X-ray spectrum. The lower panel of Figure 1 displays the hardness ratio lightcurve of the pointed PSPC observation. It suggests some spectral variability, with the spectrum becoming softer with increasing count rate.

The mean count rates measured from the EPIC PN and MOS-1 and MOS-2 observations were $0.21 \pm 0.01 \text{ cts s}^{-1}$, $0.053 \pm 0.003 \text{ cts s}^{-1}$, and $0.057 \pm 0.003 \text{ cts s}^{-1}$, respectively. No significant variability was detected during the 5ks and 9.4 ks PN and MOS coverages. Using PIMMS and the best-fit single powerlaw in the 0.2-2.0 keV range with Galactic absorption as given in Table 1 (§ 3.2) the PN and MOS count rates convert into 0.016 PSPC cts s^{-1} and 0.019 PSPC cts s^{-1} suggesting a long-term variability by factors of 3-4 in the 9 and 11 years between the XMM observation and the pointed ROSAT and RASS observations.

Converting the single powerlaw spectrum with Galactic absorption to the PN data as given in Table 1 into a PSPC hardness ratio results in $\text{HR}=0.58$, suggesting that the source has become harder compared to the pointed ROSAT PSPC observation. It agrees with the findings for the pointed PSPC lightcurve (Figure 1) that the hardness ratio increases with decreasing countrate.

3.2. Spectral analysis

The number of photons collected during the RASS coverage was only 22, not sufficient enough to perform spectral fits to the data. However, the 9 ks pointed PSPC observation was long enough

to collect 625 source photons that allow a spectral analysis. Figure 2 displays a single power law fit with neutral absorption at $z=0$ to the PSPC data of Mkn 1239. Table 1 lists the results of spectral fits to the ROSAT PSPC. The data are well-fitted by a single powerlaw with Galactic and intrinsic absorption. The X-ray spectral index is $\alpha_X=2.74 \pm 0.27$. This slope agrees in the 0.1-1.8 keV energy range with the results by using EXSAS which give $\alpha_X=2.79 \pm 0.30$ with an $N_H = 7.76 \times 10^{20} \text{ cm}^{-2}$. EXSAS has been used for the analysis of the soft X-ray selected AGN sample of Grupe et al. (2001) and Grupe et al. (2004a). The fit to the PSPC data also shows that there is excess absorption above the Galactic value ($N_H=4.03 \times 10^{20} \text{ cm}^{-2}$; Dickey & Lockman (1990)). For consistency reasons (see discussion § 4.1) we also fitted an absorbed powerlaw to the ROSAT PSPC data in the 0.1-2.4 keV range, which results in an X-ray index $\alpha_X=2.97 \pm 0.30$.

A single powerlaw fit to the XMM EPIC PN and MOS data in the 0.2-2.0 keV ROSAT PSPC energy range confirms the steep X-ray spectrum with $\alpha_X=2.95 \pm 0.24$ (Table 1). The fit shows strong residuals around 0.9 keV. This spectral feature can be fitted by a single Gaussian emission line with an equivalent width of $\text{EW}=120 \text{ eV}$ which significantly improves the fit. Fig. 3 displays this fit to the XMM PN and MOS data. Even though the PN has the best energy resolution close to the CAMEX at 0.9 keV (c.f. Ehle et al. (2003)) the line is not resolved. The fit to the MOS data results in equivalent widths of 150 eV and 110 eV for the MOS1 and MOS2, respectively. Theoretically, the energy resolution of the MOS cameras is better than the PN. However, because the source is rather faint, the MOS data had to be rebinned which reduces the resolution and the line is not resolved either. The line seems to be real and not an effect of the detectors or a result of mis-calibration, because i) no features in the EPIC detectors around this energy are known, ii) it can be seen in all three XMM detectors, iii) it can also be seen in the residuals of the ROSAT PSPC spectrum (Fig. 2), and iv) there are emission lines around this energy that have been found in the X-ray spectral of several AGN (see discussion § 4.3).

Even though the 0.2-2.0 keV range seems to be well-fitted by an absorbed powerlaw model with

³ $\text{HR}=(\text{H}-\text{S})/(\text{H}+\text{S})$ with S counts in the 0.1-0.4 keV range and $\text{H}=0.5-2.0 \text{ keV}$

a Gaussian emission line, the spectrum becomes more complicated when seen in the 0.2-12 keV range as displayed in Figure 4. A simple absorbed powerlaw model fails to fit the data above 2 keV. The spectral fit still results in a steep X-ray spectral index $\alpha_X \approx 2.7$, but the fit is not acceptable (Table 2). Even though it results in an acceptable fit, an approach with a broken powerlaw model fails because it needs an un-physically flat hard X-ray component with $\alpha_X = -2.1$. The high degree of optical polarization in Mkn 1239 (Goodrich 1989; Brindle et al. 1990) suggests that part of the observed emission is scattered while another part of the direct light path is highly absorbed. Having this in mind, we fitted a powerlaw model with two absorbers to the data. The result of this fit is shown in Figure 5. This improves the fit to $\chi^2/\nu = 38.3/50$. Figure 6 displays the unfolded spectrum of this fit showing the soft and hard X-ray continuum components and the Gaussian line at 0.91 keV. This result is somewhat similar what has been seen in the Seyfert 1.5 galaxy Mkn 6 (Feldmeier et al 1999; Immler et al. 2003). The two absorber model is identical to a partial covering model in which the partially covered continuum component passes a second absorber. It can be interpreted either as a leaky absorber or an additional line of sight through a scattering medium (see § 4.2). Partial covering models have been successfully fitted to the XMM data of NLS1s, such as 1H0707-495 (Boller et al. 2002) and IRAS 13224-3809 (Boller et al. 2003).

As shown in Figure 5 there are still some residuals around 6.5 keV suggesting the presence of a Fe K α line complex. Adding an additional Gaussian to the data results in a line with an equivalent width EW=1.3keV, but the quality of the data does not allow to constrain any of the line parameters.

3.3. Spectral Energy Distribution

Fig. 7 displays the Spectral Energy Distribution (SED) of Mkn 1239. Radio observations of Mkn 1239 have been published by Ulvestad et al. (1995); Rush et al. (1996b), and Thean et al. (2000) showing a compact radio source. In the plot we used the values of Ulvestad et al. (1995). The far infrared luminosities were derived from the IRAS point source catalogue and the near infrared data were taken from the 2 Micron All-Sky

Survey (2MASS). The optical spectrum was observed in 1997 at McDonald Observatory (Grupe et al. 1998b) and the UV spectrum was from an IUE observation of Mkn 1239 (SWP 33659) derived from the IUE archive at VILSPA. The X-ray data are represented by the un-absorbed powerlaw model that was fitted to the EPIC PN data in the 0.2-2.0 keV energy range (Table 1).

One of the crucial points in determining the SED of this highly reddened AGN is de-reddening. For the optical and UV data we used the values given in Table 1 in Gaskell et al. (2003). For the UV we used a fixed ratio $A_\lambda/A_V = 1.44$ and for the optical wavelength range we determined $A_\lambda/A_V = 1.9762 - 1.7724 \times 10^{-4} \times \lambda$ with λ in units of Å. For the 2MASS data we used $A_\lambda/A_V = 0.68 \times (1/\lambda - 0.35)$ with λ in units of μm (Ward et al. (1980)).

The 6cm radio flux density which is used for the definition of the radio loudness (Kellermann et al. 1989) is 19.49 ± 1.05 mJy and 25.9 ± 1.3 mJy (Ulvestad et al. (1995) and Rush et al. (1996b), respectively). Using the definition of Kellermann et al. (1989) with R^4 for radio-loud sources and the de-reddened flux density at 4400Å the radio loudness becomes $R = 5.3$ and 7.0 , respectively. This would make Mkn 1239 a radio-quiet source. Nevertheless it is a borderline object between radio-loud and radio-quiet.

We determined the X-ray loudness α_{ox} ⁵ using the unabsorbed monochromatic luminosities $L_{2500\text{Å}}$ and $L_{2\text{keV}}$ which were measured directly from the SED given in Fig. 7. This results in $\alpha_{\text{ox}} = 1.50$. This agrees almost perfectly with the value of α_{ox} given by Yuan et al. (1998) for a source of a redshift $z < 0.2$ and an optical luminosity density $\log l_{\text{opt}} = 23$ [W Hz⁻¹] (30 [ergs s⁻¹ Hz⁻¹]).

From the best-fit two absorber powerlaw model given in table 2 we estimated the unabsorbed 0.2-2.0 rest-frame X-ray luminosity $\log L_{0.2-2.0\text{keV}} = 37.27$ [W] (44.27 [ergs s⁻¹]) and the 0.2-12 keV rest-frame luminosity $\log L_{0.2-12.0\text{keV}} = 37.29$ [W] (44.29 [ergs s⁻¹]) which makes Mkn 1239 one of the high-luminous NLS1s compared with the sample of Grupe et al. (2004a). The contri-

⁴Radio loudness $R = F_{5\text{GHz}}/F_{4400\text{Å}}$ > 10

⁵ α_{ox} is the slope of a hypothetical power-law from 2500 Å to 2 keV; $\alpha_{\text{ox}} = 0.384 \log (L_{2500}/L_{2\text{keV}})$

bution of the soft, scattered component is $\log L_{0.2-12\text{keV}}(\text{soft}) = 35.00$ [W] (42.00 [ergs s⁻¹]). This is about 1/200th of the unabsorbed total X-ray luminosity in the 0.2-12 keV band and agrees well with the covering fraction of 0.995% found when a partial covering absorption model was used to fit the data. The monochromatic luminosity at 5100\AA is $\log \lambda L_{5100} = 36.90$ [W] (43.90 [ergs s⁻¹]). With a $\text{FWHM}(\text{H}\beta) = 1050 \text{ km s}^{-1}$ and the relations given in Kaspi et al. (2000) we estimated the mass of the central black hole to $M_{\text{BH}} = 5 \times 10^6 M_{\odot}$. This converts to an Eddington luminosity of $\log L_{\text{Edd}} = 37.7$ [W] (44.7 [ergs s⁻¹]). From the SED the bolometric luminosity was estimated to $\log L_{\text{bol}} \approx 38.0$ [W] by using a powerlaw with exponential cutoff plus soft X-ray powerlaw with neutral absorption to model the Big Blue Bump emission as described by Grupe et al. (2004a). This suggests that Mkn 1239 has an Eddington ratio L/L_{Edd} of about 2.

4. Discussion

4.1. The steep X-ray slope α_X

The soft X-ray spectrum with $\alpha_X \approx 3.0$ is unusually steep even for a NLS1, but not uncommon (e.g. Boller et al. (1996) and Grupe et al. (2001)). Its black hole mass of $5 \times 10^6 M_{\odot}$ and Eddington accretion ratio L/L_{Edd} of about 2-3 are similar to what has been found for other NLS1s (e.g. Grupe et al. (2004a) and Grupe (2004)). With an $\alpha_X = 2.97$ and a $\text{FWHM}(\text{H}\beta) = 1050 \pm 150 \text{ km s}^{-1}$ (Grupe et al. 1998b), Mkn 1239 is one of the extreme sources in a $\text{FWHM}(\text{H}\beta)$ - α_X -diagram (c.f. e.g. Boller et al. (1996); Grupe et al. (1999); Grupe (2004); Williams et al. (2002)). Figure 8 displays the position of Mkn 1239 (marked as the large star) in the $\text{FWHM}(\text{H}\beta)$ - α_X diagram of the complete soft X-ray selected sample of Grupe et al. (2004a) and Grupe (2004). The value taken for this plot was $\alpha_X = 2.97$ to be consistent with the other objects for which EXSAS had been used for the ROSAT data analysis. Please note, that Mkn 1239 is the only NLS1 in this plot that was not selected by X-rays.

4.2. Partial covering and its relation to optical polarization

The degree of optical polarization is wavelength dependent and increases with decreasing wave-

length (Goodrich 1989; Brindle et al. 1990) suggesting two main light paths between the continuum source and the observer, one direct, highly reddened absorbed light path and one indirect scattered and less-absorbed light path. The XMM data seem to confirm this model. The best-fit model to the PN data contains a powerlaw with two absorbers (Table 2). We interpret the soft component not as direct light from a leaky absorber situation, but rather as a scattered component. This interpretation is motivated by the high degree of optical polarization. This picture is somewhat similar to the model proposed by Feldmeier et al (1999) based on ASCA observations of Mkn 6 which was confirmed by the XMM observation (Immler et al. 2003).

Smith et al. (2004) have noticed that the polarization in the $\text{H}\alpha$ line shows a minimum of polarization in the blue wing, while the polarization in the red wing shows a peak. Therefore, Smith et al. (2004) concluded that the scattering medium is part of the nuclear outflow. A strong outflow is expected in a sources with high L/L_{Edd} (e.g. King & Pounds (2003)) like Mkn 1239.

4.3. The strong NeIX emission line

One of our main findings in the X-ray spectrum of Mkn 1239 is a strong emission feature around 0.9 keV. Given the energy of the feature, the most obvious identifications would be the Ne IX triplet. However, the strength of the line, and the lack of any other detectable emission features, is surprising. In the first case, the absence of the oxygen triplet is unexpected. For solar metal abundances that lines are expected to be stronger than the Neon features. Taking the line parameters of the 0.91 keV feature, we found an upper limit for the 22\AA OVII triplet of an equivalent widths $\text{EW} = 34\text{\AA}$. An identification of the line with Neon would thus lead us back to speculations about a neon/oxygen overabundance first discussed in the context of PG1404+226 (Komossa & Fink 1998; Ulrich et al. 1999). In the latter case, features were seen in absorption, while we detect an emission-line in Mkn 1239. Note that Ne and/or Fe-L lines are relatively stronger to oxygen in AGN with steep X-ray spectra (c.f. Nicastro et al. (1999)). A possible origin of that line then is the ionized medium not located along the line-of-sight, thus seen in emission.

The presence of He-like ions like NeIX in emission suggests a hot plasma with temperature of several million K (e.g. Pradhan (1982); Porquet & Dubau (2000); Porquet et al. (2001) and Ness et al. (2003) and references therein). These type of emission lines have been found in the X-ray spectra of hot stars (e.g. Audard et al. (2001); Stelzer et al. (2002) and Ness et al. (2003)), and have also been reported for a few AGN, e.g. NGC 3783 (Kaspi et al. 2002; Krongold et al. 2003), NGC 1068 (Kinkhabwala et al. 2002), NGC 5548 (Kaastra et al. 2000) and NGC 4151 (Ogle et al. 2000). The 0.91 keV line found in Mkn 1239 from the XMM data show an EW \approx 120 eV. Comastri, et al. (1998) reported of a strong NeIX line in the ASCA spectrum of the Seyfert 2 galaxy NGC 4507 with a similar equivalent width as found in Mkn 1239. The continuum spectrum of NGC 4507 is somewhat similar to Mkn 1239 in showing a highly absorbed hard X-ray component and a less absorbed soft component. In both cases, emission lines are strongly detected because the direct light is suppressed. Theoretically the presence of an He-like ion triplet provides a powerful tool to determine parameters of the plasma such as electron temperature and density (e.g. Netzer (1996)) Unfortunately in the case of Mkn 1239 the source is too faint to be explored by XMM's RGS. Much more powerful observatories such as XEUS and CON-X have to be used to observe this source with high resolution X-ray spectrometers.

4.4. X-ray variability

The variability of a factor of about 4 between the pointed ROSAT PSPC and the XMM observation about 9 years later cannot be explained only by a change in the intrinsic absorption column. Using the changes in the absorption columns of the ROSAT PSPC and XMM observations as given in Table1 would only cause a variability by a factor of about 2. This means that the source has to be variable intrinsically. Changes in the observed X-ray flux by factors of 3-4 are not uncommon among AGN (e.g. Leighly (1999); Grupe et al. (2001) and references therein), especially NLS1s (e.g. Boller et al. (1996)). The fits to the PSPC and XMM data in the 0.2-2.0 keV energy range do not suggest any significant change in the soft X-ray slope (Table 1). From the current data sets, the fits are consistent with a spectrum that goes

just up and down without any significant changes of its spectral slope α_X .

5. Conclusions

We have studied the X-ray spectra of Mkn 1239 in a serendipitous observation by XMM and our three main results are:

1. The 0.2-2.0 keV soft X-ray spectrum of the source is very steep with $\alpha_X \approx 3.0$ confirming previous results from ROSAT.
2. The 0.2-12 keV EPIC PN X-ray continuum spectrum is best-fitted by a powerlaw with $\alpha_X = 2.92$ and two intrinsic absorbers with $N_H = 6 \times 10^{20} \text{cm}^{-2}$ and $3 \times 10^{23} \text{cm}^{-2}$, supporting the optical spectropolarimetry results by Goodrich (1989) of having a direct highly absorbed light path and an indirect scattered light path which is less absorbed.
3. The X-ray spectrum shows an emission line feature around 0.91 keV (observed frame) which is most likely the NeIX triplet.
4. The non-detection of the OVII triplet suggests a super-solar Ne/O ratio.
5. To finally resolve the 0.91 keV feature, longer observations with XMM or even more powerful future X-ray missions are needed.

We would like to thank Michael Freyberg and Frank Haberl for intensive discussions about the EPIC PN and MOS calibration. Many thanks also to Anil Pradhan for discussion on Helium-like ions and Joe Shields for helpful comments and discussions. This research has made use of the NASA/IPAC Extra-galactic Database (NED) which is operated by the Jet Propulsion Laboratory, Caltech, under contract with the National Aeronautics and Space Administration. The ROSAT project is supported by the Bundesministerium für Bildung und Forschung (BMBF/DLR) and the Max-Planck-Society. This work was supported in part by NASA grant NAG5-9937.

REFERENCES

- Audard, M., Behar, E., Güdel, M., Raassen, Porquet, D., Mewe, R., Foley, C.R., & Bronage, G.E., 2001, A&A, L329

- Beuermann, K., Thomas, H.-C., Reinsch, K., et al., 1999, *A&A*, 347, 47
- Boller, T., Brandt, W.N., & Fink, H.H., 1996, *A&A*, 305, 53
- Boller, T., Fabian, A.C., Sunyaev, R., et al., 2002, *MNRAS*, 329, 1
- Boller, T., Tanaka, Y., Fabian, A., et al., 2003, *MNRAS*, 343, 89
- Boroson, T.A., & Green, R.F., 1992, *ApJS*, 80, 109
- Boroson, T.A., 2002, *ApJ*, 565, 78
- Brindle, C., Hough, J.H., Bailey, J.A., Axon, D.J., Ward, M.J., Sparks, W.B., & McLean, I.S., 1990, *MNRAS*, 244, 577
- Comastri, A., Vignali, C., Cappi, M., Matt, G., Audano, R., Awaki, H., & Ueno, S., 1998, *MNRAS*, 295, 443
- Dickey, J.M., & Lockman, F.J., 1990, *ARA&A*, 28, 215
- Ehle, M., Breittellner, M., Gonzales Riestra, R., et al., 2003, *XMM-Newton Users' Handbook*, Issue 2.1
- Feldmeier, J.J., Brandt, W.N., Elvis, M., Fabian, A.C., Iwasawa, K., & Mathur, S., 1999, *ApJ*, 510, 167
- Gaskell, C.M., Goosmann, R.W., Antonucci, R.R.J., & Whyson, D., 2003, *ApJ* submitted, astro-ph/0309595
- Goodrich, R.W., 1989, *ApJ*, 342, 224
- Grupe, D., 1996, PhD Thesis, Universität Göttingen
- Grupe, D., 2004, *AJ*, accepted, astro-ph/0401167
- Grupe, D., Beuermann, K., Thomas, H.-C., Mannheim, K., & Fink, H.H., 1998, *A&A* 330, 25
- Grupe, D., Wills, B.J., Wills, D., Beuermann, K., 1998, *A&A*, 333, 827
- Grupe, D., Beuermann, K., Mannheim, K., & Thomas, H.-C., 1999, *A&A*, 350, 805
- Grupe, D., Thomas, H.-C., & Beuermann, K., 2001, *A&A*, 367, 470
- Grupe, D., Wills, B.J., Leighly, K.M., & Meusinger, H., 2004a, *AJ*, 127, 156
- Immler, S., Brandt, W.N., Vignali, C., Bauer, F.E., Crenshaw, D.M., Feldmeier, J.J., & Kraemer, S.B., 2003, *AJ*, 126, 153
- Jansen, F., Lumb, D., Altieri, B., et al., 2001, *A&A*, 365, L1
- Kaastra, J.S., Mewe, R., Liedahl, D.A., Komossa, S., & Brinkmann, A.C., 2000, *A&A*, 354, L83
- Kaspi, S., Smith, P.S., Netzer, H., Moaz, D., Januzzi, B.T., & Giveon, U., 2000, *ApJ*, 533, 631
- Kaspi, S., Brandt, W.N., George, I.M., et al., 2002, *ApJ*, 574, 643
- Kellermann, K.I., Sramek, R., Schmidt, M., Shaffer, D.B., & Green, R., 1989, *AJ*, 98, 1195
- King, A.R., & Pounds, K.A., 2003, *MNRAS*, 345, 657
- Kinkhabwala, A., Sako, M., Behar, E., et al., 2002, *ApJ*, 575, 732
- Komossa S., & Fink H., 1998, in: *Highlights in X-ray astronomy*, B. Aschenbach & M.J. Freyberg (eds.), MPE Report 272, 147
- Krongold, Y., Nicastro, F., Brickhouse, N.S., Elvis, M., Liedahl, D.A., & Mathur, S., 2003, *ApJ*, 597, 832
- Laor, A., Fiore, F., Elvis, M., Wilkes, B.J., & McDowell, J.C., 1994, *ApJ*, 435, 611
- Laor, A., Fiore, F., Elvis, M., Wilkes, B.J., & McDowell, J.C., 1997, *ApJ*, 477, 93
- Leighly, K.M., 1999, *ApJS*, 125, 317
- Leighly, K.M., Mushotzky, R.F., Nandra, K., & Forster, K., 1997, *ApJ*, 489, L25
- Leighly, K.M., Kay, L.E., Wills, B.J., Wills, D., & Grupe, D., 1997, *ApJ*, 489, L137
- Ness, J.-U., Brickhouse, N.S., Drake, J.J., & Huenemoerder, D.P., 2003, *ApJ*, 598, 1277
- Netzer, H., 1996, *ApJ*, 473, 781

- Nicastro F., Fiore F., Matt G., 1999, ApJ, 517, 108
- Ogle, P.M., Marshall, H.L., Lee, J.C., & Canizares, C.R., 2000, ApJ, 545, L81
- Osterbrock, D.E., & Pogge, R.W., 1985, ApJ, 297, 166
- Pfefferkorn, F., Boller, T., & Rafanelli, P., 2001, A&A, 368, 797
- Pfeffermann, E., Briel, U.G., Hippmann, H., et al., 1987, SPIE, 733, 519
- Porquet, D., & Dubau, J., 2000, A&AS, 143, 495
- Porquet, D., Mewe, R., Dubau, J., Raassen, A.J.J., Kaastra, J.S., 2001, A&A, 376, 1113
- Pradhan, A., 1982, ApJ, 263, 477
- Rush, B., Malkan, M.A., Fink, H.H., & Voges, W., 1996, ApJ, 471, 190
- Rush, B., Malkan, M.A., & Edelson, R.A., 1996, ApJ, 473, 130
- Schwope, A.D., Hasinger, G., Lehmann, I., et al., 2000, AN, 321, 1
- Smith, J.E., Robinson, A., Alexander, D.M., Young, S., Axon, D.J., & Corbett, E.A., 2004, MNRAS, accepted, astro-ph/0401496
- Stelzer, B., Burwitz, V., Audard, M., et al., (2002), A&A, 392, 585
- Strüder, L., Briel, U., Dennerl, K., et al., 2001, A&A, 365, L18
- Sulentic, J.W., Zwitter, T., Marziani, P., & Dultzin-Hacyan, D., 2000, ApJ, 536, L5
- Thean, A., Pedlar, A., Kukula, M.J., Baum, S.A., & O’Dea, C.P., 2000, MNRAS, 314, 573
- Thomas, H.-C., Beuermann, K., Reinsch, K., et al., 1998, A&A, 335, 467
- Trümper, J., 1982, Adv. Space Res., 4, 241
- Turner, M.J.L., Abbey, A., Arnaud, M., et al., 2001, A&A, 365, L27
- Ulrich M.-H., Comastri A., Komossa S., Crane P., 1999, A&A, 350, 816
- Ulvestad, J.S., Antonucci, R.R.J., & Goodrich, R.W., 1995, AJ, 109, 81
- Vaughan, S., Edelson, R., Warwick, R.S., Malkan, M.A., & Goad, M.R., 2001, MNRAS, 327, 673
- Voges, W., Aschenbach, B., Boller, T., et al., 1999, A&A, 349, 389
- Ward, M., Penston, M.V., Blades, J.C., & Turtle, A.J., 1980, MNRAS, 193, 563
- Williams, R.J., Pogge, R.W., & Mathur, S., 2002, AJ, 124, 3042
- Wills, B.J., Wills, D., Evans, N.J., Natta, A., Thompson, K.L., Breger, M., & Sitko, M.L., 1992, ApJ, 400, 96
- York et al., 2000, AJ, 120, 1579
- Yuan, W., Brinkmann, W., Siebert, J., Voges, W., 1998, A&A, 330, 108
- Yuan, M.J., & Wills, B.J., 2003, ApJ, 593, L11
- Zimmermann, U., Boese, G., Becker, W., et al., 1998, 'EXSAS User’s Guide', MPE report (<http://wave.xray.mpe.mpg.de/exsas/users-guide>)

This 2-column preprint was prepared with the AAS L^AT_EX macros v5.2.

TABLE 1

SPECTRAL FIT PARAMETERS TO THE EPIC PN AND MOS AND ROSAT PSPC DATA OF MKN 1239 IN THE ROSAT PSPC 0.1-2.0 KEV ENERGY RANGE.

Detector	XSPEC Model	$N_{\text{H,gal}}$ 10^{20}cm^{-2}	$N_{\text{H,intr}}$ 10^{20}cm^{-2}	α_{X}	EW(NeIX) Å	χ^2 (DOF)
PSPC ¹	wa po ³	7.77±0.95	—	2.73±0.27	—	23.0 (28)
	wa zwa po ⁴	4.03 (fix)	3.91±1.00	2.74±0.29	—	23.0 (28)
PN ²	wa po ³	10.94±2.07	—	2.95±0.24	—	47.7 (45)
	wa zwa po ⁴	4.03 (fix)	7.47±2.21	2.97±0.25	—	47.5 (45)
	wa po gaus ⁵	9.75±1.95	—	2.94±0.24	120	34.7 (42)
MOS-1+MOS-2 ²	wa po ³	16.50±3.99	—	3.34±0.36	—	53.0 (42)
	wa zwa po ⁴	4.03 (fix)	14.15±4.45	3.44±0.38	—	52.6 (42)
	wa po gaus ⁵	12.02±3.87	—	3.04±0.35	153, 104	37.4 (37)
PN+MOS-1+MOS-2 ²	wa po ³	13.60±2.15	—	3.14±0.21	—	98.2 (86)
	wa zwa po ⁴	4.03 (fix)	10.07±2.41	3.21±0.23	—	97.5 (86)
	wa po gaus ⁵	10.41±1.59	—	2.94±0.18	120, 150, 110	74.4 (84)

¹ROSAT PSPC, observed energy range 0.1-1.8 keV

²EPIC PN, MOS-1 and MOS-2observed energy range 0.2-2.0 keV

³galactic absorption and powerlaw model

⁴galactic absorption, redshifted neutral absorption at z=0.02 and powerlaw

⁵powerlaw with Galactic absorption and Gaussian line at ≈ 0.92 keV

TABLE 2

SPECTRAL FIT PARAMETERS TO THE EPIC PN 0.2-12 KEV DATA OF MKN 1239. THE GALACTIC N_{H} IS FIXED FOR ALL MODELS TO $4.03 \cdot 10^{20}\text{CM}^{-2}$.

Parameter	Models		
	ZWA PO ¹	ZWA(PO+GA) ²	ZWA(PO+GA)+ZWA(PO) ³
Absorber 1, N_{H} [10^{20}cm^{-2}]	5.76±1.82	5.06±1.81	6.21±2.01
Absorber 2, N_{H} [10^{22}cm^{-2}]	—	—	33.24±13.46
Spectral index α_{X}	2.75±0.20	2.75±0.20	2.92±0.23
Gauss line, E [keV]	—	0.913±0.022	0.913 (fix)
Gauss line, σ [eV]	—	32.4 ^{+61.0} _{-32.4}	32.4 (fix)
Gauss line, EW [eV]	—	110	110 (fix)
χ^2/ν	111.9 (53)	99.6 (50)	38.3 (50)

¹XSPEC model ZWA PO, intrinsic absorption by neutral elements and powerlaw

²XSPEC model ZWA(PO+GAUS), intrinsic absorption with powerlaw and Gaussian emission line

³XSPEC model ZWA (PO+GAUS) + ZWA (PO), Two-component intrinsic absorption with powerlaw and Gaussian line

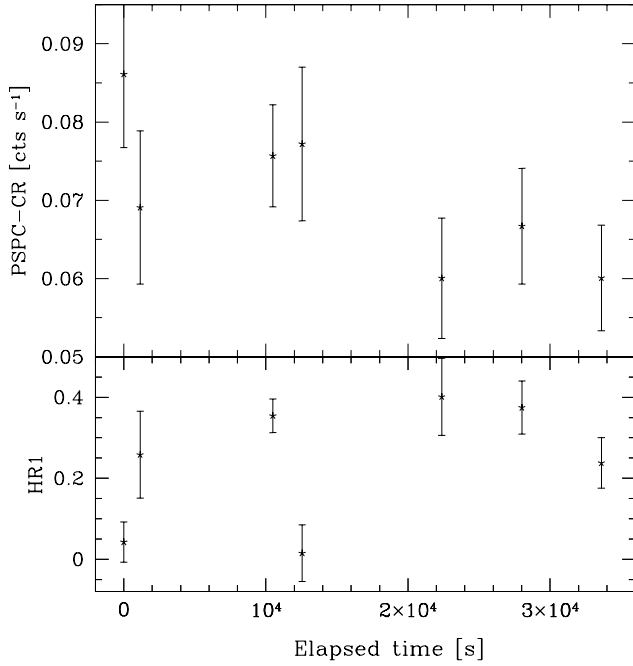


Fig. 1.— Light curve of the pointed ROSAT PSPC observation of Mkn 1239. The upper panel shows the count rate vs. elapsed time and the lower panel displays the variability of the hardness ratio.

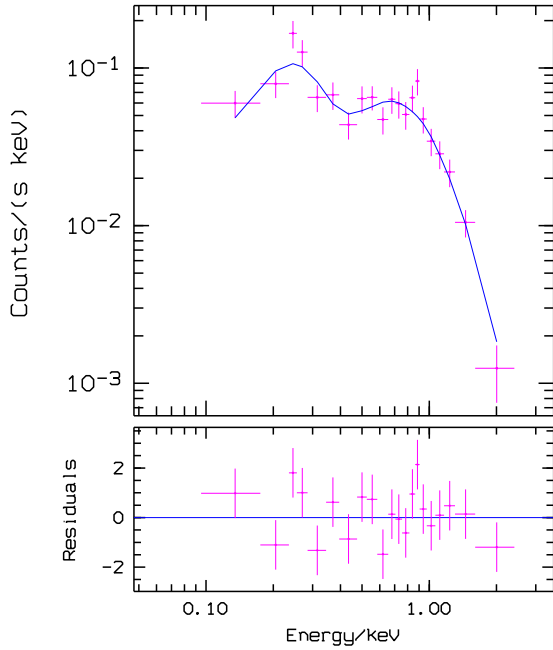


Fig. 2.— Single Power law fit to the pointed PSPC spectrum of Mkn 1239 with absorption at $z=0.0$.

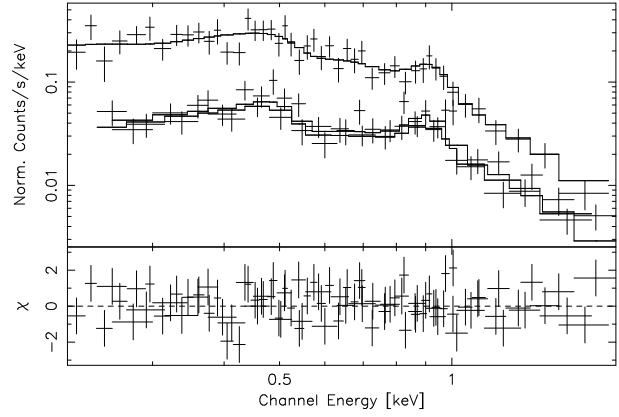


Fig. 3.— Powerlaw fit with Galactic absorption and Gaussian line at 0.9 keV to the XMM EPIC PN and MOS spectra in the 0.2-2.0 keV energy range (Table 1).

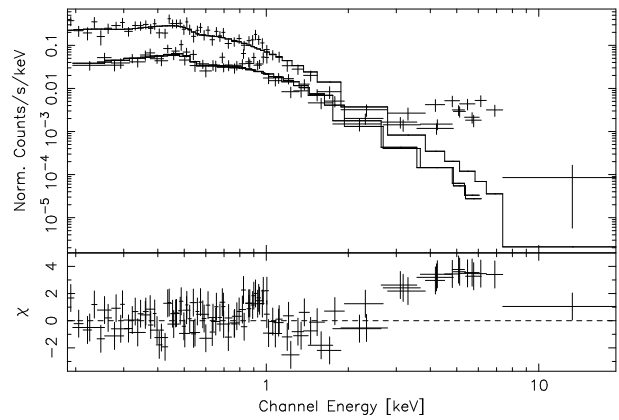


Fig. 4.— Power law fit with Galactic and intrinsic absorption fit to the XMM EPIC PN and MOS data of Mkn 1239. The plot shows that the simple powerlaw that fits the soft energy range, does not fit the entire spectrum.

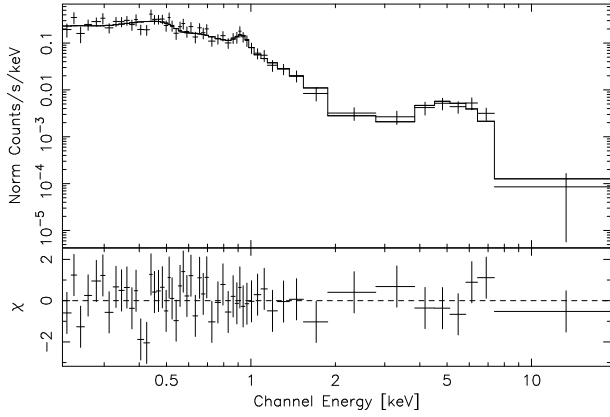


Fig. 5.— Spectral fit with a powerlaw model and two intrinsic absorbers and a Gaussian line to the PN data of Mkn 1239 (see Table 2).

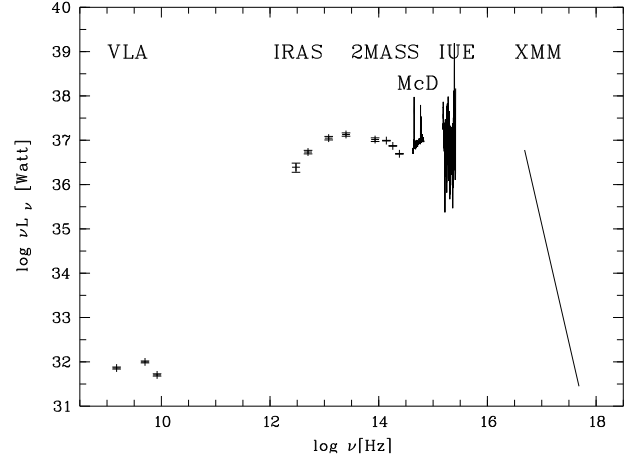


Fig. 7.— Spectral Energy Distribution of Mkn 1239. The NIR, optical and UV data are corrected for reddening. The XMM data are represented by an unabsorbed powerlaw of the EPIC PN observation in the 0.2-2.0 keV range as given in Tab. 1.

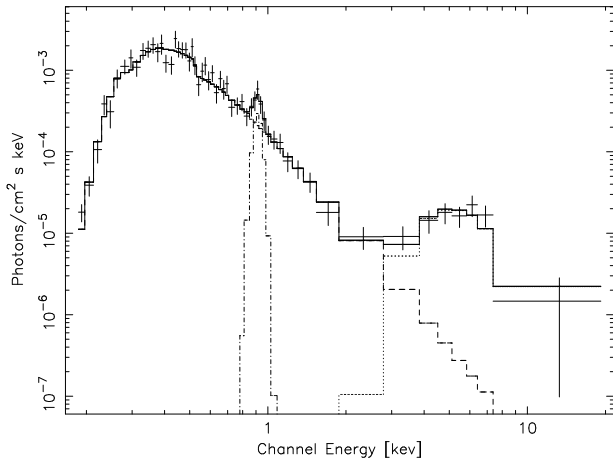


Fig. 6.— Unfolded spectrum with a powerlaw model and two intrinsic absorbers and a Gaussian line to the PN data of Mkn 1239 (see Figure 5; Table 2).

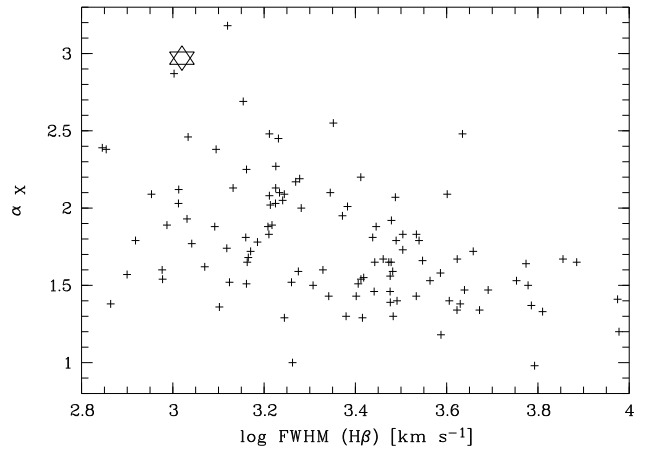


Fig. 8.— FWHM($H\beta$) - α_X diagram of the soft X-ray selected AGN sample of Grupe et al. (2004a) and Grupe (2004). The position of Mkn 1239 is marked by the star.